EPJ Web of Conferences **274**, 04002 (2022) https://doi.org/10.1051/epjconf/202227404002
XVth Quark Confinement and the Hadron Spectrum

Massive lighter quark corrections to boosted-top cross section

Alejandro Bris[1,3,*], *Vicent* Mateu[2,**], and *Fernando* Gil[4,***]

[1]Departamento de Física Teórica, Universidad Autónoma de Madrid,
E-28049, Madrid, Spain
[2]Departamento de Física Fundamental e IUFFyM, Universidad de Salamanca,
E-37008 Salamanca, Spain
[3]Instituto de Física Teórica UAM-CSIC,
E-28049 Madrid, Spain
[4]Instituto de Física Corpuscular UV-CSIC,
E-46980 Valencia, Spain

Abstract. In this work we present the computation of the missing pieces to get the bHQET thrust distribution with non-vanishing secondary quark masses at NNLO: the jet and hard functions. The difference with respect to the massless case is encoded in diagrams with massive-quark bubbles. For its computation we use a Mellin Barnes representation of the dispersive integral method that permits expressing the result as an analytic, fast-converging expansion in powers of a small parameter rather than integrals that can only be solved numerically. We also obtain the matching coefficient present when integrating out the quark mass. It is necessary for a continuous top-down running and to verify the consistency check.

1 Introduction

The peak region in top quark production at colliders is best described in boosted heavy quark effective theory, where its mass is integrated out. Within this framework one has the following factorization theorem for the thrust differential cross section in e^+e^--collisions [1, 2]:

$$\frac{1}{\sigma_0}\frac{\mathrm{d}\sigma_{\mathrm{bHQET}}}{\mathrm{d}\tau} = Q^2 H(Q,\mu_M) H_M\Big(M,\frac{Q}{M},\mu_M,\mu\Big)\int \mathrm{d}\ell\, B_\tau\Big(\frac{Q^2(\tau-\tau_{\min})-Q\ell}{M},\mu\Big) S_\tau(\ell,\mu)\,, \quad (1)$$

$$B_\tau(\hat{s},\mu) = M\int_0^{\hat{s}} \mathrm{d}\hat{s}'\, B_n(\hat{s}-\hat{s}',\mu) B_n(\hat{s}',\mu)\,,$$

where M is the mass of the primary quark, Q the center-of-mass energy and $\tau_{\min} = 2(M/Q)^2$. Large logarithms are summed up by evolving the matrix elements from their respective natural scales to a common μ, with the running setup sketched in Fig. 1

The Hard H and Soft S_τ functions are the same as those in SCET and can be found at

*e-mail: alejandro.bris@uam.es
**e-mail: vmateu@usal.es
***e-mail: Fernando.Gil@ific.uv.es

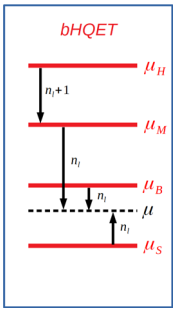

Figure 1: Running setup for bHQET considering only primary quark mass. μ_H, μ_M, μ_B and μ_S are the natural scales corresponding to the matrix elements H, H_M, B_τ and S_τ respectively. μ is the final common scale and n_l is the number of massless flavours. Next to each arrow is indicated the number of active flavours in that patch.

NNLO in [3] and [4], respectively. Furthermore, the Hard function is the square of QCD-SCET matching coefficient so it does not depend on the secondary quark mass and the corrections to the Soft function are already known [5]. Therefore we only need to compute the missing corrections for the Hard H_M and Jet B_τ functions

2 bHQET with massive secondary quark

Considering a non-vanishing secondary quark mass brings a richer structure of effective field theories, analogous to the one presented in [6] for secondary massive quark production in SCET with massless primary quarks. We now have different scenarios depending on the hierarchy of the secondary quark mass scale μ_m with respect to the matrix-element natural scales, as shown in Fig. 2.

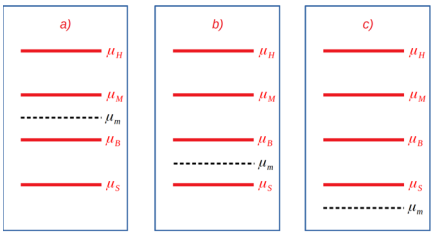

Figure 2: Different scenarios for various secondary quark masses within the bHQET framework. μ_m is the scale corresponding to secondary quark mass. The relevant scenario in the case of top (bottom) primary (secondary) quark is *b*.

On the other hand, when a matrix element runs below μ_m the secondary quark is integrated out to avoid large logs and therefore does not participate in the evolution, leading to a flavour matching coefficient for the matrix element when passing through the scale μ_m. In addition, due to the freedom in choosing a final common scale μ, we also have consistency conditions between factorization formulas including flavour matching, as for instance the one depicted in Fig. 3 for scenario *b*.

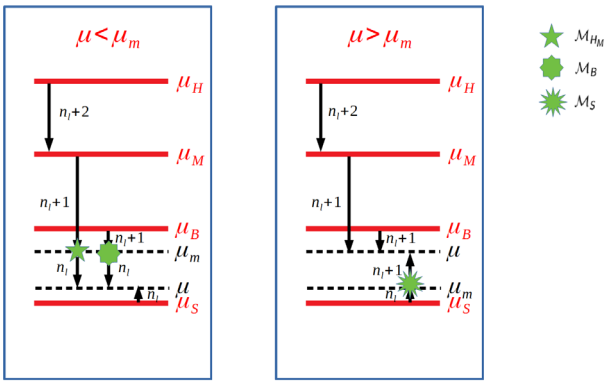

Figure 3: Consistency condition for scenario *b*. Both running setups must yield the same result.

3 Dispersive integral method

Secondary quark mass corrections involve two loop Feynman diagrams with a massive bubble insertion. The computation of such diagrams is carried out using a dispersive integral method, that consists in writing the massive bubble as the integral over an effective gluon propagator. Therefore we perform the one-loop computation with a modified gluon, followed by the dispersive integral.

In the usual approach, the massive bubble is cast as an integral over a massive gluon propagator:

$$\text{massive-bubble} \longrightarrow \frac{-i}{p^2}\left(g^{\mu\nu} - \frac{p^\mu p^\nu}{p^2}\right)\Pi(p^2, m^2)\,, \tag{2}$$

$$\frac{\Pi(p^2,m^2)-\Pi(0,m^2)}{p^2} = T_F\frac{\alpha_s}{4\pi}\int_{4m^2}^{\infty} \mathrm{d}\tilde{m}^2\,\frac{\mathcal{V}^{(d)}(\tilde{m},\mu)}{p^2-\tilde{m}^2+i\epsilon}\,,$$

$$\mathcal{V}^{(d)}(\tilde{m},\mu) = \frac{8\Gamma(2-\varepsilon)}{\Gamma(4-2\varepsilon)}\frac{\beta_{\tilde{m}}}{\tilde{m}^2}\left(\frac{4\pi\tilde{\mu}^2}{\beta_{\tilde{m}}^2\tilde{m}^2}\right)^{\varepsilon}\left(1-\varepsilon+\frac{2M^2}{\tilde{m}^2}\right),$$

where m is the secondary-quark mass, $\beta_{\tilde{m}} \equiv \sqrt{1-4M^2/\tilde{m}^2}$, $d = 4-2\varepsilon$, and $\tilde{m}$ the gluon effective mass.

On the other hand, using the Mellin-Barnes representation for the modified gluon propagator reduces the complexity to massless 1-loop with modified exponents:

Starting from a closed expression for $\Pi(p^2, m^2)$:

$$\Pi(p^2,m^2) = \frac{T_F\,\Gamma(\varepsilon)}{2\varepsilon-3}\frac{\alpha_s}{\pi}\left(\frac{4\pi\tilde{\mu}^2}{m^2}\right)^{\varepsilon}\left[\left(1-\varepsilon+\frac{2m^2}{p^2}\right){}_2F_1\left(1\,,\,\varepsilon\,;\,\frac{3}{2}\,;\,\frac{p^2}{4m^2}\right)-\frac{2m^2}{p^2}\right] \tag{3}$$

we write the hypergeometric function as an integral:

$${}_2F_1\left(1\,,\,\varepsilon\,;\,\frac{3}{2}\,;\,\frac{p^2}{4m^2}\right) = \frac{\Gamma(3/2)}{\Gamma(\varepsilon)\,\Gamma(3/2-\varepsilon)}\int_0^1 \mathrm{d}x\,\frac{x^{-1+\varepsilon}(1-x)^{1/2-\varepsilon}}{1-\frac{p^2}{4m^2}\,x}\,, \tag{4}$$

and use Mellin-Barnes representation:

$$\frac{1}{1-\frac{p^2}{4m^2}\,x} = \frac{1}{2\pi i}\int_{c-i\infty}^{c+i\infty}\mathrm{d}h\left(-\frac{p^2}{4m^2}\,x\right)^{-h}\Gamma(h)\,\Gamma(1-h)\,. \tag{5}$$

The x integral can be carried out right away and one finds:

$$\frac{\Pi(p^2,m^2)-\Pi(0,m^2)}{p^2}=\frac{T_F\,\alpha_s}{2\pi^2 i p^2}\left(\frac{4\pi\tilde{\mu}^2}{m^2}\right)^{\varepsilon}\int_{c-i\infty}^{c+i\infty}\mathrm{d}h\left(-\frac{m^2}{p^2}\right)^{-h}\frac{1+h}{3+2h}\frac{h\Gamma^2(h)\Gamma(1-h)\Gamma(h+\varepsilon)}{\Gamma(2h+2)}\,. \tag{6}$$

Therefore we obtain the following modified gluon propagator:

$$\frac{-ig^{\mu\nu}}{p^2}\longrightarrow\frac{ig^{\mu\nu}}{(-p^2)^{1-h}}\,, \tag{7}$$

which does not introduce an additional energy scale in one-loop computations. Moreover, it is the same modification found in large-β_0 computations. Also, integration of h by residues yields directly expansions for large or small masses (through the converse mapping theorem) and one even may get closed forms in terms of Meijer G-functions. On the contrary, employing directly the dispersive integral method may require extra effort when dealing with distributions, and computing its cumulative may become necessary.

4 Matrix Elements

4.1 Jet Function

As shown in Eq. (1), the thrust Jet function B_τ is the result of convolving two hemisphere jet functions B_n. The latter can be obtained as the imaginary part of a forward-scattering matrix element:

$$\mathcal{B}_n(\hat{s},\mu)=\frac{i}{4\pi N_C M}\,\mathrm{Tr}\left[\int\mathrm{d}^d x\,e^{ikx}\left\langle 0\middle|\,T\left\{\,W_n^+(x)\,h_v(x)\;\bar{h}_v(0)\,W_n(0)\right\}\middle|0\right\rangle\right], \tag{8}$$

$$B_n(\hat{s},\mu)=\mathrm{Im}\Big[\mathcal{B}_n(\hat{s},\mu)\Big],$$

where W_n are Wilson lines with ultra-collinear gluons and h_v is the heavy quark field.

One-loop results

The non-vanishing Feynman diagrams we need to consider, with the corresponding modified gluon propagator in each case, are shown in Fig. 4. For the massive gluon propagator we

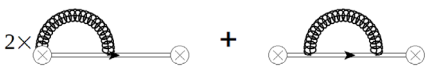

Figure 4: One-loop Feynman diagrams for Jet function.

obtain the following result:

$$B_n(\hat{s},\mu,\tilde{m})=\frac{\alpha_s C_F}{4\pi M}\left\{2\,\Gamma(\varepsilon)\left(\frac{\mu^2}{\tilde{m}^2}e^{\gamma}\right)^{\varepsilon}\left[\left(-H_{\varepsilon-1}+2\log(\tilde{m})+1\right)\delta(\hat{s})-2\left[\frac{\theta(\hat{s})}{\hat{s}}\right]_+-\frac{2\tilde{m}\pi^{1/2}\,\Gamma(1/2+\varepsilon)}{(2\varepsilon-1)\,\Gamma(\varepsilon)}\,\delta'(\hat{s})\right]\right.$$
$$\left.+\,\theta\left(\hat{s}^2-4\tilde{m}^2\right)\left[\frac{8}{\hat{s}}\log\left(\frac{\hat{s}+\sqrt{\hat{s}^2-4\tilde{m}^2}}{2\tilde{m}}\right)-\frac{4\sqrt{\hat{s}^2-4\tilde{m}^2}}{\hat{s}^2}\right]+O(\varepsilon)\right\} \tag{9}$$

which reproduces the known massless jet function of Ref. [1]. For the gluon propagator in Eq. (7), the result reads:

$$B_n^h(\hat{s},\mu)=-C_F\frac{\alpha_s}{\pi M}\frac{\Gamma(2+h-\varepsilon)\,\hat{s}^{-1+2h}e^{\varepsilon\gamma_E}}{(\varepsilon-h)\Gamma(1-h)\Gamma(2+2h-2\varepsilon)}\left(\frac{\mu}{\hat{s}}\right)^{2\varepsilon}\,, \tag{10}$$

in agreement with [7].

Final result

After carrying out renormalization we get for the thrust jet function with massive secondary quark the following result:

$$B_\tau^{(n_l+1)}(\hat{s},\mu,m) = B_\tau^{(n_l+1)}(\hat{s},\mu) + \delta B_m^{dist}(\hat{s},\mu,m) + \delta B_m^{real}(\hat{s},m)\,, \tag{11}$$

$$\begin{aligned}
\delta B_m^{dist}(\hat{s},\mu,m) =& \left(\frac{\alpha_s^{(n_l+1)}}{4\pi}\right)^2 \frac{C_F}{M}\left[\left(\frac{32}{9}L_m^3 + \frac{128}{9}L_m^2 + \left(\frac{976}{27} - \frac{16\pi^2}{9}\right)L_m + \frac{3568}{81} - \frac{64\pi^2}{27} - \frac{32}{3}\xi_3\right)\delta(\hat{s})\right.\\
&\left. + \left(\frac{16\pi^2}{9} - \frac{32}{3}L_m^2 - \frac{256}{9}L_m - \frac{976}{27}\right)\mathcal{L}^0(\hat{s}) + \left(\frac{64}{3}L_m + \frac{256}{9}\right)\mathcal{L}^1(\hat{s}) - \frac{32}{3}\mathcal{L}^2(\hat{s}) - 8\pi^2 m\,\delta'(\hat{s})\right],\\
\delta B_m^{real}(\hat{s},m) =& \left(\frac{\alpha_s^{(n_l+1)}}{4\pi}\right)^2 \frac{C_F}{M}\,\frac{\theta\left(\hat{s}^2-16m^2\right)}{\hat{s}}\left[\frac{976}{27} - \frac{16\pi^2}{9} + \frac{256}{9}\log\left(\frac{m}{\hat{s}}\right) + \frac{32}{3}\log^2\left(\frac{m}{\hat{s}}\right)\right.\\
&\left. + \sum_{n=0}^{\infty}\frac{\left[\left(\frac{1}{2}\right)_n\right]^2}{(n!)^2(n+2)^3}\left(\frac{4n-1}{n+2} + 2(1+2n)\left[\psi(n+1) - \psi(n+1/2) - \log\left(\frac{4m}{\hat{s}}\right)\right]\right)\left(\frac{16m^2}{\hat{s}^2}\right)^{2+n}\right]\\
=& \left(\frac{\alpha_s^{(n_l+1)}}{4\pi}\right)^2 \frac{C_F}{M}\,\frac{2\pi}{\hat{s}}\,G_{5,5}^{5,0}\left(\frac{16m^2}{\hat{s}^2}\,\middle|\,\begin{matrix}1,1,1,\frac{3}{2},\frac{5}{2}\\ 0,0,0,2,2\end{matrix}\right),
\end{aligned}$$

where $B_\tau^{(n_l+1)}(\hat{s},\mu)$ is the jet function with massless secondary quarks that can be found in [8], and $L_m \equiv \log\left(\frac{m}{\mu}\right)$ and $\mathcal{L}^i(\hat{s}) \equiv \frac{1}{\mu}\left[\frac{\theta(\hat{s})\log^i(\hat{s}/\mu)}{\hat{s}/\mu}\right]_+$.

4.2 bHQET Hard Function

It is defined as the square of the matching coefficient between SCET and bHQET currents, which can be computed as the ratio of the corresponding form factors in each theory:

$$C_M = \frac{\langle q,\bar{q}|\mathcal{J}_{\rm SCET}|0\rangle}{\langle q,\bar{q}|\mathcal{J}_{\rm bHQET}|0\rangle} = \frac{F_{\rm SCET}}{F_{\rm bHQET}}\,, \qquad H_M = |C_M|^2\,, \tag{12}$$

One-loop results

The terms that contribute are shown in Fig. 5.

The SCET form factor with a massive gluon propagator $F_{\rm SCET}^{\tilde{m}}$ is already known and can be

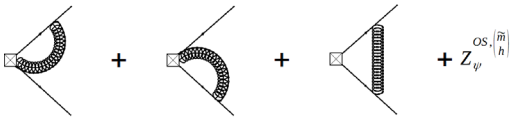

Figure 5: One-loop contributions to form factors in SCET and bHQET.

found in [9] whereas in bHQET we get:

$$F_{\rm bHQET}^{\tilde{m}} = \frac{\alpha_s C_F}{2\pi}\Gamma(\varepsilon)\left(\frac{\mu^2}{\tilde{m}^2}e^{\gamma}\right)^{\varepsilon}\left[1 + \log\left(\frac{M^2}{Q^2}\right) + i\pi\right]. \tag{13}$$

Regarding the gluon propagator in Eq. (7), the bHQET form factor is scaleless and vanishes in dimensional regularization ($F_{\rm bHQET}^{h} = 0$) while the SCET result is:

$$F_{\rm SCET}^{h} = \frac{\alpha_s C_F}{\pi}\left(\mu^2 e^{\gamma}\right)^{\varepsilon}(h-1)\left(1 + \frac{(3-2\varepsilon)(\varepsilon-h-1)(\varepsilon-h)}{2+h-2\varepsilon}\right)\frac{\Gamma(\varepsilon-h)\Gamma(2h-2\varepsilon)}{\Gamma(2+h-2\varepsilon)}M^{2h-2\varepsilon}. \tag{14}$$

Final result

$$
\begin{aligned}
C_M^{(n_l+1)}\left(M,\frac{Q}{M},\mu,m\right) &= C_M^{(n_l+1)}\left(M,\frac{Q}{M},\mu\right)+\delta C_M\left(\frac{m}{M}\right), \qquad (15)\\
\delta C_M\left(\frac{m}{M}\right) &= \left(\frac{\alpha_s^{(n_l+1)}}{4\pi}\right)^2 C_F T_f\left\{\frac{1747}{81}+\frac{52\pi^2}{27}+\left(\frac{532}{27}+\frac{16}{9}\pi^2\right)\hat{L}_m+\frac{104}{9}\hat{L}_m^2+\frac{32}{9}\hat{L}_m^3\right.\\
&\quad+\frac{1}{2}\int_{4m^2}^{\infty}\mathrm{d}\tilde{m}^2\,\mathcal{V}^{(4)}(\tilde{m},\mu)\left[\frac{\left(-\beta_{\tilde{m}}^3-5\beta_{\tilde{m}}+6\right)}{\beta_{\tilde{m}}(\beta_{\tilde{m}}+1)^2}\log\left(\frac{1-\beta_{\tilde{m}}}{2}\right)-\frac{\left(\beta_{\tilde{m}}^3+5\beta_{\tilde{m}}+6\right)}{(1-\beta_{\tilde{m}})^2\beta_{\tilde{m}}}\log\left(\frac{\beta_{\tilde{m}}+1}{2}\right)\right.\\
&\quad\left.\left.+\frac{\beta_{\tilde{m}}^2-25}{2\left(1-\beta_{\tilde{m}}^2\right)}+4\log\left(\frac{1-\beta_{\tilde{m}}}{2}\right)\log\left(\frac{\beta_{\tilde{m}}+1}{2}\right)\right]\right\}\\
&=\left(\frac{\alpha_s^{(n_l+1)}}{4\pi}\right)^2 C_F T_f\left[6\pi^2\frac{m}{M}+\frac{4m^2}{M^2}\left(6+8\hat{L}_m\right)-\frac{110}{9}\pi^2\frac{m^3}{M^3}\right.\\
&\quad\left.+\frac{m^4}{3M^4}\left(145+12\pi^2-72\left(2-\hat{L}_m\right)\hat{L}_m\right)+\frac{m^6}{M^6}\sum_{n=0}^{\infty}a_n(m/M)\left(\frac{m^2}{M^2}\right)^n\right],\\
a_n(m/M) &= \frac{8}{(n+1)(n+2)(n+3)^3(2n+3)(2n+5)}\left[506+750n+413n^2+100n^3+9n^4\right.\\
&\quad+\left(408+778n+589n^2+221n^3+41n^4+3n^5\right)\log(4)+(n+2)(n+3)(n+4)\left(17+14n+3n^2\right)\\
&\quad\left.\times\left[2\hat{L}_m+\psi(-1/2-n)+\psi(1+n)-2\psi(7+2n)\right]\right],
\end{aligned}
$$

where $C_M^{(n_l+1)}\left(M,\frac{Q}{M},\mu\right)$ is the secondary massless quark matching coefficient that can be found in [9] and $\hat{L}_m \equiv \log\left(\frac{m}{M}\right)$

5 Flavour matching

The various flavor matching conditions were obtained in a way analogous to the one described in [6]. They quantify the gap in a matrix element when integrating out the secondary quark so we have:

$$
\mathcal{M}_B = M\int \mathrm{d}\hat{s}'\, B_\tau^{(n_l)}(\hat{s}-\hat{s}',\mu_m,m)\left[B_\tau^{(n_l+1)}(\hat{s}',\mu_m,m)\right]^{-1}, \qquad (16)
$$

$$
\mathcal{M}_{C_M} = \frac{C_M^{(n_l)}\left(M,\frac{Q}{M},\mu_m,m\right)}{C_M^{(n_l+1)}\left(M,\frac{Q}{M},\mu_m,m\right)} \;;\quad \mathcal{M}_{H_M} = \left|\mathcal{M}_{C_M}\right|^2 .
$$

5.1 Jet Function

The bHQET Jet function below the secondary quark mass scale can be written as the sum of the massless Jet function and the corresponding bubble diagrams with the subtraction of the renormalization constant in the on-shell scheme:

$$
B_\tau^{(n_l)}(\hat{s},\mu,m) = B_\tau^{(n_l)}(\hat{s},\mu)+B_\tau^{m-\text{bubble},OS}(\hat{s},\mu,m)-Z_B^{OS}\left(\hat{s},\mu,m\right). \qquad (17)
$$

The renormalization constant can be determined from the decoupling condition, which in this case is the following:

$$
\lim_{m\to\infty}\left[B_\tau^{(n_l)}(\hat{s},\mu,m)\right] = B_\tau^{(n_l)}(\hat{s},\mu)-\left(\frac{\alpha_s}{4\pi}\right)^2\frac{C_F}{M}\,8\pi^2 m\,\delta'(\hat{s}), \qquad (18)
$$

where the second term comes from n_l-bHQET Lagrangian due to the fact that when integrating out massive secondary quark bubbles, they remain as a contribution to the primary quark self-energy:

$$\mathcal{L}_{\text{bHQET}^{(n_l)}} = \bar{h}_v \left[i\, v \cdot \mathrm{D} - \delta M - \left(\frac{\alpha_s}{4\pi}\right)^2 C_F\, 2\pi^2 m \right] h_v \,. \tag{19}$$

All in all we get:

$$\begin{aligned} \mathcal{M}_B(\hat{s},\mu,m) = & \left(\frac{\alpha_s^{(n_l+1)}}{4\pi}\right)^2 \frac{C_F}{M} \left\{ \left[-\frac{32}{9} L_m^3 - \frac{128}{9} L_m^2 + \left(-\frac{688}{27} + \frac{4\pi^2}{9}\right) L_m - \frac{440}{27} + \frac{5\pi^2}{27} \right.\right. \\ & \left.\left. + \frac{28}{9}\xi_3 \right] \delta(\hat{s}) + \left(\frac{32}{3} L_m^2 + \frac{160}{9} L_m + \frac{224}{27}\right) \mathcal{L}^0(\hat{s}) \right\}. \end{aligned} \tag{20}$$

5.2 bHQET Hard Function

For the n_l bHQET matching coefficient one has:

$$C_M^{(n_l)}\left(M, \frac{Q}{M}, \mu, m\right) = C_M^{(n_l)}\left(M, \frac{Q}{M}, \mu\right) + C_M^{m-\text{bubble},OS}\left(M,\mu,m\right) - Z_{C_M}^{OS}\left(M,\mu,m\right), \tag{21}$$

but now it is necessary to remove secondary quark contribution also from the running of SCET Hard function H when taking decoupling limit:

$$\lim_{m\to\infty}\left[H^{(n_l+2)}(Q,\mu,m)\, H_M^{(n_l)}\left(M, \frac{Q}{M}, \mu, m\right)\right] = H^{(n_l+1)}(Q,\mu)\, H_M^{(n_l)}\left(M, \frac{Q}{M}, \mu\right). \tag{22}$$

Therefore using the following expression for $H^{(n_l+1)}$:

$$H^{(n_l+1)}(Q,\mu) = \lim_{m\to\infty}\left[|\mathcal{M}_C(Q,\mu,m)|^2\; H^{(n_l+2)}(Q,\mu,m)\right], \tag{23}$$

fixes the condition for the renormalization constant:

$$2\mathrm{Re}\left[C_M^{m-\text{bubble},OS}\left(M,\mu,m\right) - Z_{C_M}^{(2\text{-loop}),OS}\left(M,\mu,m\right) - \mathcal{M}_C^{(2\text{-loop})}(Q,\mu,m)\right] \underset{m\to\infty}{\longrightarrow} 0\,, \tag{24}$$

where $\mathcal{M}_C(Q,\mu,m)$ is the flavour matching for the QCD-SCET Wilson coefficient that can be found in [6]. Taking everything into account the result is:

$$\mathcal{M}_{H_M}^{(2)}\left(M, \frac{Q}{M}, \mu_m, m\right) = \left(\frac{\alpha_s^{(n_l+1)}}{4\pi}\right)^2 C_F\, \frac{16}{27}\left[9\log^2\left(\frac{m}{\mu_m}\right) + 15\log\left(\frac{m}{\mu_m}\right) + 7\right]\left[1 - 2\log\left(\frac{Q}{M}\right)\right]. \tag{25}$$

6 Preliminary Numerical Results

Combining all pieces of the factorization theorem one gets the thrust bHQET distribution. We have implemented the results in a numerical code. To that end we follow the steps that appear in Ref. [10] for the bHQET thrust differential cross-section at N^{3}LL + $O(\alpha_s^2)$ with massless secondary quarks and added the massive corrections. To get a taste of the size of these corrections we show in Figs. 6 and 7 some numerical results for top-quark production with massive secondary bottom quarks.

We took the following values for the center-of-mass energy, top quark mass and top width: $Q = 2000\,\text{GeV}$, $M_t^{\text{pole}} = 170.034\,\text{GeV}$ and $\Gamma_t = 1.32\,\text{GeV}$.

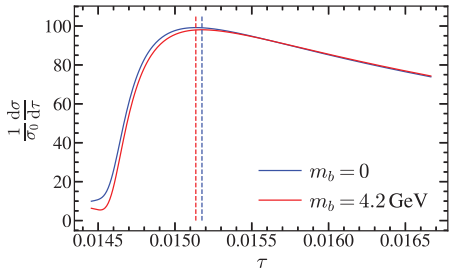

Thrust distributions for massless and massive secondary quark

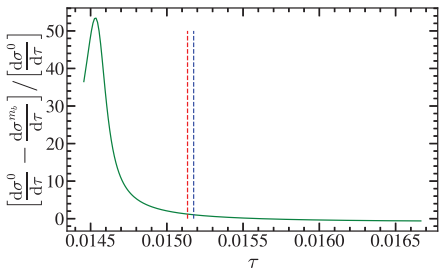

Percentage of relative difference between massless and massive distributions.

Figure 6: In this plot m_b is the value of the bottom mass in GeV units and dashed lines mark the corresponding peak position.

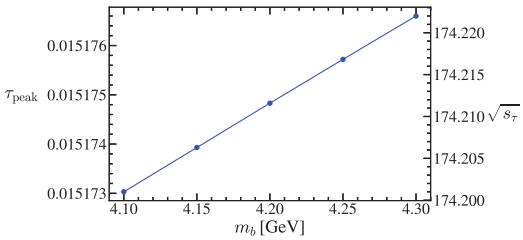

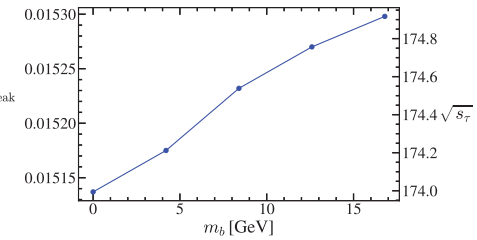

Figure 7: Peak position for the thrust distributions as a function of the bottom mass in GeV units. We also show the corresponding value for the hemisphere jet invariant mass $\sqrt{s}$.

References

[1] S. Fleming, A.H. Hoang, S. Mantry, I.W. Stewart, Phys. Rev. D **77**, 114003 (2008)
[2] S. Fleming, A.H. Hoang, S. Mantry, I.W. Stewart, Phys. Rev. D **77**, 074010 (2008)
[3] R.N. Lee, A.V. Smirnov, V.A. Smirnov, JHEP **04**, 020 (2010), 1001.2887
[4] P.F. Monni, T. Gehrmann, G. Luisoni, JHEP **08**, 010 (2011), 1105.4560
[5] S. Gritschacher, A. Hoang, I. Jemos, P. Pietrulewicz, Phys. Rev. D **89**, 014035 (2014), 1309.6251
[6] P. Pietrulewicz, S. Gritschacher, A.H. Hoang, I. Jemos, V. Mateu, Phys. Rev. D **90**, 114001 (2014), 1405.4860
[7] N.G. Gracia, V. Mateu, JHEP **07**, 229 (2021), 2104.13942
[8] A. Jain, I. Scimemi, I.W. Stewart, Phys. Rev. D **77**, 094008 (2008), 0801.0743
[9] A.H. Hoang, A. Pathak, P. Pietrulewicz, I.W. Stewart, JHEP **12**, 059 (2015), 1508.04137
[10] B. Bachu, A.H. Hoang, V. Mateu, A. Pathak, I.W. Stewart, Phys. Rev. D **104**, 014026 (2021), 2012.12304